Comparison of the Diagnostic Performance of Changes in Signal Intensity and Volume From Multiparametric MRI for Assessing Response of Rectal Cancer to Neoadjuvant Chemoradiotherapy

Zhengwu Tan
Wuhan Union Hospital
Lan Zhang
Huazhong University of Science and Technology Tongji Medical College First Clinical College: Wuhan Union Hospital
Lan Cheng
Huazhong University of Science and Technology Tongji Medical College First Clinical College: Wuhan Union Hospital
Lingling Xie
Huazhong University of Science and Technology Tongji Medical College First Clinical College: Wuhan Union Hospital
Zhenyu Lin Lin
Huazhong University of Science and Technology Tongji Medical College First Clinical College: Wuhan Union Hospital
Ping Han
Huazhong University of Science and Technology Tongji Medical College First Clinical College: Wuhan Union Hospital
Xin Li (lxwsry2014@163.com)
Huazhong University of Science and Technology Tongji Medical College First Clinical College: Wuhan Union Hospital

Research

Keywords: chemoradiotherapy (CRT), complete response (CR), magnetic resonance imaging (MRI), locally advanced rectal cancer (LARC), tumor volumetry

Posted Date: June 15th, 2021

DOI: https://doi.org/10.21203/rs.3.rs-598039/v1

Abstract

Background: Tumor regression grade (TRG) correlates with prognosis in patients with locally advanced rectal cancer (LARC), but there is controversy regarding the use of magnetic resonance imaging (MRI) for determining TRG. This study to evaluate the diagnostic value of change rate in signal intensity (SI) and volume (V) from MRI to TRG following preoperative chemoradiotherapy (CRT) in patiens with LARC.

Materials and methods: This retrospective analysis examined 82 LARC patients who were admitted to our institution between Oct 2017 and Oct 2019. Patients underwent pre- and post-CRT T2-weighted (T2W), diffusion-weighted (DW)/apparent diffusion coefficient (ADC), and contrast-enhanced T1-weighted (ceT1W) MRI. Change rate of volume and relative SI ratio(%△V and %△SIR) from each sequence were determined. All LARCs were confirmed pathologically and classified into TRG 0, 1, 2 and 3. Descriptive statistics and receiver operating characteristic (ROC) analysis, with calculation of area under the curve (AUC), were used to compare the diagnostic performances.

Results: Sixteen patients had TRG-0, 15 had TRG-1, 35 had TRG-2, and 16 had TRG-3. Except for ADC-%△SIR, the remaining%△V and %△SIR on T1W, DWI, and ceT1W had significant differences among the four groups. %△V and/or %△SIR did not distinguish TRG-1 from TRG-2 nor TRG-2 from TRG-3, but differences between other TRGs were identified by %△V and/or %△SIR on T2W, DWI, and ceT1W. The combined use of DW-%△V and T2W-%△SIR provided the best diagnostic performance in distinguishing of TRG-0 from TRG-2 (AUC: 0.954) and from TRG-3 (AUC: 1.000).

Conclusions: Preoperative MRI of LARC patients can determine TRG and may improve selection of the preoperative therapy.

Background

The use of multiple treatment modalities for locally advanced rectal cancer (LARC) has markedly improved patient outcomes during the last three decades(1). A major reason for this improvement is the use of neoadjuvant chemoradiotherapy (CRT)(1, 2). CRT provides major benefits in terms of tumor regression grade (TRG) and tumor downsizing, factors that are significantly and independently associated with improved survival and disease-free survival (DFS)(3). For example, Huh et al. compared the prognostic significance of TRG in patients with rectal cancer after preoperative CRT and found better 5-year overall survival (OS) and DFS in patients with TRG0 (complete response) than in those with TRG1 (moderate), and TRG2–3 (minimal–poor)(4). Suzuki et al. used a modified classification system based on pathological T (ypT) stage and TRG, and showed that a less advanced stage was independently related to improved DFS(5). Assessment of preoperative TRG after CRT may help to stratify patients according to prognosis so that clinicians can administer the most appropriate preoperative therapy(6). Therefore, it is important to determine TRG before surgery of these patients. The responses to preoperative CRT are variable, and range from pathologic complete response (pCR) to cancer progression.

Approximately 10 to 30% of rectal cancer patients achieve pCR after CRT, leading some researchers to recommend a ‘wait-and-see’ policy regarding surgery, with clinical follow-up for these patients(1, 2, 7).

Magnetic resonance imaging (MRI) is a non-invasive examination that is playing an increasingly important role in oncology, and is now the gold standard for initial staging of rectal cancer and assessment of restaging after neoadjuvant CRT(7). Several studies reported the use of TRG based on MR (mrTRG) following preoperative CRT for predicting pathological TRG (pTRG), DFS, and OS in patients with LARC(1, 6, 8–13). However, there are differences between mrTRG and pTRG, and there is no consensus on whether mrTRG can be used as a surrogate of pTRG(7, 10, 11) because it is difficult to distinguish tumors from tissue fibrosis based on MRI signal intensity (SI) after CRT(3, 14). Consequently, some studies performed quantitative analyses of MRI results with morphological evaluations to assess TRG after CRT based on tumor SI and volume (V), and showed promising results(11, 14–19). Other studies reported that tumor SI and V had some potential additional diagnostic value for patients who were pathological good responders(2, 11, 16, 20).

Previous studies examined the use tumor SI and V to discriminate pCR or other response groups from non-pCR or other nonresponsive groups(16, 21), and reported questionable performance in identification of different TRGs. There is good evidence that TRG after CRT is associated with DFS and OS in patients with LARC(4–6, 10, 13), so an accurate clinical assessment of the preoperative response is essential. However, no study has yet reported the use of quantitative multiparametric MRI to determine TRGs in LARC.

We hypothesized that relative SI (SIR) and change of V, determined by different MRI sequences before and after CRT, were associated with TRG. We therefore evaluated the diagnostic value of different MRI sequences in predicting pTRG after preoperative CRT in patients with LARC.

Methods

This retrospective study was approved by the Institutional Review Board and Research Ethics Committee of our Hospital. The need for written informed consent was waived.

Patients

Clinical data were obtained from the hospital database for 168 consecutive patients with rectal cancer who received total mesorectal resection (TME) after CRT between October 2017 and October 2019 (Fig. 1). The inclusion criteria were: histologically confirmed rectal adenocarcinoma; locally advanced disease (staged by pre-CRT MRI results as cT3–4 and/or N-category positive and/or positive extramural venous invasion and mesorectal fascia); completion of standard CRT, followed by TME; availability of pre- and post-CRT MRI results from different sequences, including T2-weighted (T2W), diffusion-weighted (DW)/apparent diffusion coefficient (ADC), non-contrast-enhanced T1-weighted (nonceT1W), and contrast-enhanced T1-weighted (ceT1W); and receipt of standard TME within 8 to 10 weeks of completing the full CRT course(21). The exclusion criteria were: non-resectable and/or metastatic

disease; insufficient quality of MRI results; tumor with signet ring cell carcinoma after TME, with several high-signal mucus components (based on T2WI) and numerous postoperative pathological mucus lakes (greater than 50%); and more than 10 weeks between post-CRT MRI and surgery. This last exclusion criterion was used because tissue changes can occur when there is a long interval between post-CRT MRI and surgery(2).

MRI protocol

Patients were examined using different MRI machines (Table 1) at 1.5 and 3.0 T with a phased array body coil and without bowel preparation. Oblique axial or axial T2W, ceT1W, and ADC images were retrieved from the Picture Archiving and Communication System (PACS, Carestream, Canada). Routine rectal MRI protocols and image acquisition parameters were used (Supplementary Table). The first MRI examination was performed to assess tumor stage, and the preoperative MRI was used to assess treatment response and restaging after CRT.

Table 1
Clinical and MRI characteristics of patients in the four TRG groups.

Characteristics		TRG 0 (16)	TRG 1 (15)	TRG 2 (35)	TRG 3 (16)	P
Gender	Male	12	12	24	13	0.74
Age, years (mean ± SD)		48.94 ± 10.22	53.20 ± 8.14	52.83 ± 10.04	50.44 ± 12.17	0.54
MRI unit	Pre- /post-CRT					0.71/0.34
	Siemens Verio	1/0	1/0	2/6	4/1	
	siemens TrioTim	2/2	0/2	4/1	3/1	
	Siemens skyra	2/1	1/2	1/3	1/1	
	Siemens Avanto	6/7	7/6	17/18	6/10	
	Siemens Aera	5/6	5/3	9/7	2/2	
	Philips Ingenia	0/0	1/1	1/0	0/1	
	GE 750w	0/0	0/1	1/0	0/0	
Tumor differentiation						0.53
	Well	0	1	4	1	
	Moderate	15	13	30	14	
	Poor	1	1	1	1	
Pre-nCRT T stage (n)						0.28
	T4	3	7	16	7	
	T3	13	8	19	9	
Post-CRT MRI restage (n)						< 0.01
	T4	0	5	5	4	
	T3	4	8	20	11	
	T2	8	2	10	1	
	T0	4	0	0	0	

Characteristics		TRG 0 (16)	TRG 1 (15)	TRG 2 (35)	TRG 3 (16)	P
Pre- to post-CRT MRI, days (mean ± SD)		91.44 ± 19.29	118.87 ± 96.29	111.49 ± 74.72	85 ± 39.1	0.36
Post-CRT MRIto surgery,days (mean ± SD)		17.25 ± 10.75	16.87 ± 12.84	16.86 ± 12.86	9.63 ± 7.58	0.16
ypT stage						< 0.01
	T4	0	2	3	4	
	T3	0	5	16	8	
	T2	0	7	14	4	
	T1	0	1	2	0	
	T0	16	0	0	0	

Evaluation of SI and V

Two gastrointestinal radiologists with expertise in rectal cancer diagnosis (7 years for one and 5 years for the other) independently calculated tumor V and SI by manually tracing the tumor boundaries on the axial images and placing free-hand regions-of-interest (ROIs), which provided the area of the lesion for each tumor-containing section (Fig. 2). Any disagreements were resolved by discussion until a consensus was achieved. On the T2W images, tumors were defined as areas of isointense or hyperintense signal relative to the hypointense signal of normal adjacent muscular rectal wall. On the DW images, areas of high SI, compared with the normal bowel wall or background of tissue with lower SI, were considered indicative of tumor; portions of the tumor with a high DW signal and a high ADC were avoided, so as to avoid T2 shine-through in the ADC data. On the ceT1W images, areas with enhanced SI relative to the normal bowel wall were considered as tumor. On post-CRT T2-weighted MRI, areas of markedly low SI at the location of the primary tumor bed were interpreted as fibrosis. Because the risk for residual tumor in these fibrotic areas may be about 50%, they were included in the measurements of V and SI(16).

Whole-tumor V was then calculated by multiplying each cross-sectional area by section thickness (Fig. 2, V1–V2). Post-CRT measurements were performed with comparison to pre-CRT images to ensure the ROIs were placed within same axial level of the location of the primary tumor. The ROIs with maximal area of tumor were obtained on single sections of axial T2W, ADC, nonceT1W, and ceTW. The intestinal lumen and artifact areas were avoided after ROI selection. In some patients, high SI zones were not identified on post-CRT DW images, in which case the ROIs were positioned at the location of the tumor bed before CRT (Fig. 3). The SI of the iliopsoas muscle (SIm) was used as reference tissue, with careful avoidance of any intramuscular fat(11, 22–24).

The Δ was defined as the absolute change in V and SI values between pre-CRT and post-CRT measurements, and %Δ as the percentage change. The formulas used to calculate T2W-%△V, DW-%△V, ceT1W-%△V, T2W-%△SIR, DW-%△SIR, and ceT1W-%△SIR are in the Supplementary Materials(16, 22, 25).

Another independent radiologist, who had 10 years of expertise in gastrointestinal diagnostics, independently assessed each pre-and post-treatment MRI result. This radiologist was blinded to the clinical, histopathological, and other characteristics of the patients.

Pathological evaluation after CRT

Surgically resected specimens were pathologically analyzed according to the seventh edition of the American Joint Committee on Cancer (AJCC) TNM staging system and the Ryan et al. staging system(26, 27). Tumor stage (T0–T4b) and pTRG were recorded. Patients were categorized based on response to therapy using a 4-point TRG system: TRG0, complete response with no viable cancer cells; TRG1, moderate response with single cancer cells or small groups of cancer cells; TRG2, minimal response with residual cancer outgrown by fibrosis; and TRG3, poor response with minimal or no tumor killing and extensive residual cancer. The our TRG assessment of the pathology system is only for the primary tumor, and the most widely used TRG systems are those of Ryan(27) for the primary tumor which has been modified by AJCC(26) with the 4-point TRG scoring system(28).

Statistical analysis

Data were expressed as numbers and percentages for categorical variables and as means ± standard deviations for continuous variables. The Kruskal-Wallis test (continuous variables) and the χ^2 test (categorical variables) were used to assess the significance of differences. The thresholds of %Δ values and different combinations for prediction of TRG were assessed using receiver operating characteristic (ROC) analysis, with identification of the best cutoff value (point nearest the upper left corner) using logistic regression analysis with the Firth bias-correction(20). Differences in diagnostic performance were determined by comparing the ROC curves using the method described by DeLong et al.(29). The κ test was used to assess agreement between post-CRT restaging MRI results and ypT stage. Five patients were randomly selected from each of the four TRG groups to evaluate inter-observer variability for two readings by calculating intraclass correlation coefficients (ICCs), which were classified as poor (0–0.2), fair (0.21–0.4), moderate (0.41–0.6), good (0.61–0.8), or excellent (0.8–1.0). Statistical analysis was performed using SPSS version 19.0, MedCalc version 19.0.4, and GraphPad Prism version 7.0. P-values were calculated using two-sided tests, and values less than 0.05 were considered significant.

Results

We enrolled 82 patients with LARC who fulfilled the inclusion and exclusion criteria. The average age was 51.67 years (± 10.16, range: 27–71) and there were 61 men (74.4%) and 21 women (25.6%).

Patient and treatment characteristics

There were 16 patients (19.5%) with TRG0, 15 patients (18.3%) with TRG1, 35 patients (42.7%) with TRG2, and 16 patients (19.5%) with TRG3 (Table 1). These groups had no significant differences in gender, age, MRI machine used for examination, tumor differentiation, pre-CRT T stage, time between pre- and post-CRT MRI, and time between post-CRT restaging MRI and surgery. The median time between pre- and post-CRT MRI was 92.5 days (range: 31–498) and the median time between restaging MRI and surgery was 12 days (range: 1–63). All patients were staged using MRI pre-CRT as cT3 (59.8%) or cT4 (40.2%).

The TRG groups had significant differences in post-CRT MRI T restage and ypT stage (both $P < 0.001$), but with low inter-observer agreement ($\kappa = 0.191$). In particular, post-CRT MRI T restaging showed that 43.9% of all tumors were downstaged, but ypT staging indicated that 70.73% of all tumors were downstaged (Table 2).

Table 2
Agreement of post-CRT clinical T restagewith ypT stage.

post-CRT	ypT stage				
T restage	Yp T0	Yp T1	Yp T2	Yp T3	Yp T4
cT 0	4	0	0	0	0
cT 1	0	0	0	0	0
cT 2	8	2	4	7	0
cT 3	4	1	18	19	1
cT 4	0	0	3	3	8

%△V and %△SIR from T2W, DW, and ceT1W sequences

Except for ADC-%△SIR, the remaining %△V and %△SIR from the T1W, ADC/DWI, ceT1W sequences had significant differences among the four TRG groups (Table 3, Fig. 4). In particular, the T2W-%△V, DW-%△V, ceT1W-%△V, T2W-%△SIR, and ceT1W-%△SIR values declined as the TRG grade declined from 0 to 3.

Table 3
Comparison of %△V and %△SIR values from the T1W, ADC/DWI, and ceT1Wsequences in the fourTRG groups.

Parameter	TRG 0(%)	TRG 1(%)	TRG 2(%)	TRG 3(%)	P
T2W-%△V	86.01 ± 15.33	43.73 ± 31.31	37.48 ± 31.53	23.27 ± 27.79	< 0.01
DW-%△V	88.89 ± 12.95	54.62 ± 31.13	42.54 ± 24.63	32.63 ± 29.70	< 0.01
ceT1W%△V	81.99 ± 14.93	48.81 ± 22.37	39.06 ± 25.84	22.30 ± 28.45	< 0.01
T2W-%△SIR	44.73 ± 8.95	29.39 ± 13.28	6.85 ± 38.31	0.2 ± 32.12	< 0.01
ADC-%△SIR	−301.19 ± 880.12	−16.24 ± 51.95	−72.94 ± 401.05	−41.9 ± 111.42	0.78
ceT1W-%△SIR	34.02 ± 36.18	17.62 ± 32.76	−11.42 ± 53.09	−26.67 ± 40.74	< 0.01

Diagnostic performance for TRG

We performed ROC analysis to compare the diagnostic performance of different values (T2W-%△V, DW-%△V, ceT1W-%△V, T2W-%△SIR, ceT1W-%△SIR, and DW-%△V*T2W-%△SIR) in predicting pTRG (Fig. 5 and Table 4).

Table 4
Results from receiver operating characteristic analysis of %△V and %△SIR from the T1W, ADC/DWI, ceT1W sequences for discrimination of different TRGs.

	AUC	Cutoff (%)	SENS (%)	SPEC (%)	ACC(%)	PPV (%)	NPV (%)	P
TRG 0 vs.**TRG 1**								
T2W-%△V	0.92(0.77,0.99)	77.59	75.00	100	87.10	100	78.95	< .01
DW-%△V	0.93(0.78,0.99)	83.72	81.25	100	90.32	100	83.33	< .01
ceT1W%△V	0.93(0.77,0.99)	77.54	75.00	100	87.10	100	78.95	< .01
TRG 0 vs.**TRG 2**								
T2W-%△V	0.94(0.83,0.99)	61.61	93.75	85.71	88.24	75.00	96.77	< .01
DW-%△V	0.95(0.85,0.99)	72.02	93.75	94.29	94.12	88.24	97.06	< .01
ceT1W%△V	0.94(0.84,0.99)	69.43	87.50	97.14	94.12	93.33	94.44	< .01
T2W-%△SIR	0.90(0.78,0.96)	29.39	100	74.29	82.35	64.00	100	< .01
ceT1W-%△SIR	0.75(0.61,0.86)	−6.42	100	54.29	68.63	50.00	100	.01
DW-%△V * T2W-%△SIR	0.95(0.86,0.99)	0.38	93.75	97.14	96.08	93.75	97.14	< .01
TRG 0 vs.**TRG 3**								
T2W-%△V	0.98(0.86,1.00)	62.78	93.75	100	96.88	100	94.12	< .01
DW-%△V	0.98(0.86,1.00)	68.64	93.75	100	96.88	100	94.12	< .01
ceT1W%△V	0.98(0.86,1.00)	60.40	93.75	100	96.88	100	94.12	< .01
T2W-%△SIR	1.00(0.89,1.00)	26.72	100	100	100	100	100	< .01
ceT1W-%△SIR	0.86(0.69,0.96)	−9.23	100	81.25	90.63	84.21	100	< .01
DW-%△V * T2W-%△SIR	1.00(0.98, 1.00)	−0.12	100	100	100	100	100	< .01
TRG 1 vs.**TRG 3**								
T2W-%△SIR	0.90(0.74,0.98)	24.98	73.33	100	87.1	100	80.00	< .01
ceT1W-%△SIR	0.82(0.64,0.93)	−11.68	86.67	81.25	83.87	81.25	86.67	< .01

AUC, area under the receiver operating curve; PPV, positive predictive value; NPV, negative predictive value; SENS, sensitivity; SPEC, specificity; ACC, accuracy.

There was excellent diagnostic performance for T2W-%△V, DW-%△V, and ceT1W-%△V in distinguishing TRG0 and TRG1 (AUC = 0.921 ~ 0.933, sensitivity = 75.00 ~ 81.28%, specificity = 100%, p < 0.001). There was good-to-excellent diagnostic performance for T2W-%△V, DW-%△V, ceT1W-%△V, T2W-%△SIR, ceT1W-%△SIR in distinguishing TRG0 and TRG2 (AUC = 0.895 ~ 0.954, sensitivity = 87.50 ~ 100%, specificity = 54.49 ~ 97.14%, p < 0.001) and in distinguishing TRG0 and TRG3 (AUC = 0.859 ~ 1.000, sensitivity = 93.75 ~ 100%, specificity = 81.25 ~ 100%, p < 0.05). There was good diagnostic performance for T2W-%△SIR, and ceT1W-%△SIR in distinguishing TRG1 and TRG3 (AUC = 0.817 ~ 0.900, sensitivity = 73.33 ~ 86.67%, specificity = 81.25 ~ 100%, p < 0.05). However, these parameters could not significantly distinguish TRG1 from TRG2, nor TRG2 from TRG3 (Fig. 4).

Comparison of diagnostic performance for TRG

For discriminating TRG0 from TRG2, the AUC was 0.937 (95% CI: 0.831,0.986) for T2W-%△V, 0.946 (95% CI: 0.845,0.990) for DW-%△V,0.939 (95% CI: 0.835,0.987), 0.939 (95% CI: 0.835, 0.987) for ceT1W-%△V, and 0.954 (95% CI: 0.855,0.993) for DW-%△V * T2W-%△SIR. These four parameters had sensitivity ranging from 87.5 to 100%, specificity ranging from 74.29 to 97.14, and accuracy ranging from 82.35 to 96.08% (Table 4). These values were also significantly greater than the AUC of 0.746 (95% CI: 0.605, 0.858) for ceT1W-%△SIR (p = 0.0080 ~ 0.0154). The AUC values calculated from the different parameters were not significantly different, although the AUC of DW-%△V * T2W-%△SIR was slightly higher than the AUCs of T2W-%△V, DW-%△V, and ceT1W-%△V, T2W-%△SIR for discriminating TRG0 from TRG2, and TRG0 from TRG 3.

Interobserver agreement

Our calculations of ICCs, based on data of 20 cases from two readings, indicated that all ICC values were excellent (T2W-%△V: 0.936; DW-%△V: 0.939; ceT1W-%△V: 0.911; T2W-%△SIR: 0.933; and ceT1W-%△SIR: 0.976), except for the ICC of ADC-%△SIR (0.325).

Discussion

Our purpose was to determine the value of %△V and %△SIR from multiparametric MRI, using individual sequences and sequence combinations, for predicting preoperative TRG after CRT in the patients with LARC. Our results indicated good to excellent diagnostic performance from T2W-%△V, DW-%△V, ceT1W-%△V, T2W-%△SIR, ceT1W-%△SIR, and DW-%△V * T2W-%△SIR for discriminating TRG0 from TRG1, TRG0 from TRG2, and TRG0 from TRG3; and for discriminating TRG1 from TRG3. Although our ROC analysis indicated no significant differences among these AUC values, DW-%△V * T2W-%△SIR had highest AUC values. In addition, none of the measurements were useful for distinguishing TRG1 from TRG2, nor for distinguishing TRG2 from TRG3. To the best of our knowledge, no prior studies comprehensively compared the diagnostic performances of change in V and SIR using T2W, DWI, and ceT1W MRI sequences to predict TRG in patients with LARC after CRT. Predicting preoperative TRG may help clinicians to stratify patients by prognosis and to implement optimal preoperative therapy(4).

We found a low agreement of post-CRT MR T restaging and ypT stage (κ = 0.191), consistent with the results of some prior studies that mrTRG cannot be used as a surrogate to predict pTRG(3, 7, 11). Previous research reported that MR quantitative results of tumor V and SI were important prognostic indicators for tumor change during CRT and response after CRT. In particular, van den Begen et al. and Lambregts et al. reported that visual changes in rectal tumor morphology (fibrosis) and volume occurred during CRT(14, 19). Tumor V correlated with downstaging of rectal cancer(17, 30), and Lambregts et al. reported that post-CRT DWI volumetry provided the best results for detection of patients with a CR after CRT (AUC = 0.92, sensitivity = 70%, specificity = 98%)(17). In line with previous studies, we found that tumor V had excellent diagnostic performance in discriminating TRG0 from TRG1, TRG0 from TRG2, and TRG0 from TRG3 (AUC = 0.921 ~ 0.984, sensitivity = 75 ~ 93.75%, and specificity = 85.71 ~ 100%).

Hötker et al. determined tumour volumetry from post-treatment dynamic contrast enhanced (DCE)-MRI and DW-MRI, and reported good correlations with histopathological percent tumour regression in resected specimens, and performance that was superior to post-CRT T2 tumour volumetry(11). In the present MRI study, the diagnostic performance of tumor V from DW was slightly greater than that from T2W and ceT1W, although there were no significant differences among AUC values. The better performance of DW images may be because this method provides easier recognition of viable tumor remnants, because they appear hyperintense compared with the low SI of surrounding non-neoplastic tissue. These results are in contrast with previous studies which showed that post-CRT DW MR volumetry provided excellent diagnostic performance in assessing CR (AUC = 0.93) and was significantly more accurate than T2-weighted MR volumetry(16).

CRT may lead to no change or only a slight change in tumour V in poor responders, but there may be fibrotic transformation that cannot be visually identified(31). The measured value of SIR may have different changes, because SIR and V can respond differently to CRT(22–25). Wan et al reported that T2WI SI related parameters, which had AUC ranging from 0.694 to 0.762, sensitivity from 68.2 to 77.3%, and specificity from 63.6 to 77.0%, were potential predictors for pCR in LARC patients after CRT(15). The value of intra-tumor heterogeneity evaluated by DW for predicting TRG after CRT in the lower rectum and measurements of ADC change induced by CRT may have considerable diagnostic value for the estimation of CR(25, 32). DCE-MRI in rectal cancer is promising, mainly for prediction of prognosis and assessment of response to CRT(33). Our results are in contrast with previous studies, in that we identified %ΔSIR on T2W and ceT1W as promising diagnostic tools for distinguishing CR from non-CR and TRG1 from TRG3, respectively. However, our ADC-%△SIR results were useless, and this discrepancy from published data is probably due to the use of different protocols, different methods for ROI selection, and differences in factors contributing to magnetic field inhomogeneity, such as pH, hydration status, and susceptibility effects(25, 32, 34, 35).

Previous studies used SIR and V from MRI sequences to discriminate pCR or response groups from non-pCR or nonresponsive groups, not for discrimination of different TRG groups(2, 3, 6, 11, 15, 19, 21, 25, 32, 35). In contrast, we used changes of SIR and V from T2W, DW/ADC, and ceT1W sequences to differentiate different TRGs after CRT. Our results indicated that T2W-%△V, DW-%△V, ceT1W-%△V, T2W-

%△SIR, ceT1W-%△SIR, and DW-%△V * T2W-%△SIR provided high diagnostic performances, with accuracies of 82.35 to 100%, in prediction of TRG after pCRT, better than reported in previous studies(2, 6, 14–19, 25, 27, 30, 32, 33). In discriminating TRG0 from TRG2, the AUC for ceT1W-%△SIR was significantly lower than the AUC for other sequences ($p < 0.05$). In discriminating pCR from non-pCR and TRG1 from TRG3, there were no significantly different AUC values from using different parameters. This indicates that multiple parameters provided high diagnostic performance for discriminating pCR from non-pCR and TRG1 from TRG3. DW-%△V * T2W-%△SIR had the best prediction of TRG, with AUCs of 0.954 ~ 1.000, sensitivity of 93.75%~100%, specificity of 97.14 ~ 100%, and accuracy of 96.08%~100%. %△V and %△SIR did not distinguished TRG1 from TRG 2, nor TRG2 from TRG3, possibly because there were only small differences in V and fibrotic transformation between these TRGs or because there were changes in ROI selection after CRT. The V parameter can distinguish TRG0 from TRG1, possibly because the ROI area is smaller in TRG0 than TRG1; the ROI for TRG0 has a fibrous bed but no tumor, but the ROI of TRG1 contains some tumor and some fibrous bed.

Although our results are encouraging, there were some limitations to our study. First, this was a retrospective study and there were small numbers of patients in the different TRG groups, and this could have led to selection bias. Thus, it is necessary to examine more patients and use a prospective study to confirm our results. Second, our data were from multiple MRI machines because it was collected retrospectively. However, except for the fair inter-observer correlation of TRG with ADC-%△SIR, other MRI measurements that had excellent inter-observer correlation(2, 17, 25). Previous studies reported better reproducibility of SIR than SI for several MRI sequences(2, 16, 18, 22–24, 34, 35). Moreover, Hötker et al. reported that DCE-MRI volumetry had better inter-observer agreement(11). Third, the selection of an ROI and comparison of MRI results before and after CRT was somewhat subjective; however, to overcome these limitations, we evaluated a relatively large area of cancerous tissue(32). Blazic et al. reported that the use of single-section and whole-tumor volume methods provided similar accuracy in predicting CR based on post-CRT measurement of ADC change, and that use of single sections was less time-consuming(25). Finally, there were variations in the timing between the pre- and post-CRT MRI examinations, with a large standard deviation, and no uniform and standard CRT scheme. These factors could have increased the risk of selection bias. However, we used the rate of change in V and SIR, and the degree of tumor change after CRT was incorporated into the corresponding TRG groups, and did not influence grouping of cases by TRG(15, 16).

In conclusion, despite the several limitations of this study, T2W-%△V, DW-%△V, ceT1W-%△V, T2W-%△SIR, ceT1W-%△SIR, and especially DW-%△V* T2W-%△SIR, provided good to excellent diagnostic performance regarding TRG prediction after CRT in patients with LARC. These results require confirmation by a large prospective cohort study. The advantages of establishing the preoperative TRG in these patients are that it provides more effective management that can be specifically tailored to individual patients, it provides reliable predictions of prognosis after CRT, and it may indicate the suitability of non-operable management, such as further CRT.

Abbreviations

LARC: locally advanced rectal cancer; CRT: chemoradiotherapy; TRG: tumor regression grade; SI: signal intensity; V: volume; MRI: magnetic resonance imaging; T2W: T2-weighted; DW: diffusion-weighted; ADC: apparent diffusion coefficient; ceT1W: contrast-enhanced T1-weighted; nonceT1W: non contrast-enhanced T1-weighted; △V: difference of volume between pre-CRT and post-CRT tumor; %△V: percent change of tumor V; SIt: SI of tumor; SIm: SI of muscle; SIR: tumor/muscle SI ratio; △SIR: change of SIR between pre- and post-CRT; %△SIR: percent change of SIR; ROC: operating characteristic curve; AUC: area under the curve; pCR: pathological complete remission; TME: total mesorectal excision; ROI: region-of-interest; cT: clinical tumor stage.

Declarations

Ethics approval and consent to participate

This research had a retrospective design and was approved by the Medical Ethics Committee of Tongji Medical College, Huazhong University of Science and Technology before giving a written consent in accordance with Chinese legislation as well as the Helsinki Declaration. Informed consent regarding MR examination was obtained from all subjects. All patients underwent routine rectal enhancement MRI examinations before and after CRT in the Radiology Department.

Statement

All methods were performed in accordance with relevant guidelines and regulations.

Consent for publication

Not applicable.

Availability of data and materials

The datasets used and/or analysed during the current study are available from the corresponding author on reasonable request.

Conflict of interest

None of the authors have any conflicts of interest to disclose.

Financial support

This research was supported by the National Natural Science Foundation of China (No. 81701673) and the Natural Science Foundation of Hubei Province.

Author contributions

Xin Li designed the study; Xin Li, Zhengwu Tan, Lingling Xie, and Zhenyu Lin collected the data; Lan Cheng collected MRI scanning parameters; Xin Li, Zhengwu Tan, and Lan Zhang reviewed the imaging data; Zhengwu Tan and Lan Zhang measured and analyzed the data, reviewed the charts, and interpreted the data; Xin Li and Zhengwu Tan wrote the manuscript; Ping Han modified the manuscript.

Acknowledgements

Not applicable.

References

1. Siddiqui MRS, Bhoday J, Battersby NJ, Chand M, West NP, Abulafi A-M, et al. Defining response to radiotherapy in rectal cancer using magnetic resonance imaging and histopathological scales. World Journal of Gastroenterology. 2016;22(37):8414.
2. S K, K H, N S, HJ K, MJ K, WS K, et al. T2-weighted signal intensity-selected volumetry for prediction of pathological complete response after preoperative chemoradiotherapy in locally advanced rectal cancer. European radiology. 2018;28(12):5231-40.
3. N H, Id-Orcid, C CTR, B CO, I P, MJ G, et al. MRI of Rectal Cancer: Tumor Staging, Imaging Techniques, and Management. Radiographics. 2019;39(2):367-87.
4. Huh JW, Kim HC, Kim SH, Park YA, Cho YB, Yun SH, et al. Tumor regression grade as a clinically useful outcome predictor in patients with rectal cancer after preoperative chemoradiotherapy. Surgery. 2019;165(3):579-85.
5. Suzuki T, Sadahiro S, Tanaka A, Okada K, Saito G, Miyakita H, et al. A Modified Classification of Prognostic Factors Based on Pathological Stage and Tumor Regression Grade in Patients with Rectal Cancer Who Receive Preoperative Chemoradiotherapy. Oncology. 2017;93(5):287-94.
6. K M, M S, A T, T N, N A, T F, et al. Prognostic Significance of Neoadjuvant Rectal Score and Indication for Postoperative Adjuvant Therapy in Rectal Cancer Patients After Neoadjuvant Chemoradiotherapy. In vivo (Athens, Greece). 2020;34(1):283-9.
7. F S, G B, D C, A W, LST M, S B, et al. Comparison between MRI and pathology in the assessment of tumour regression grade. Br J Cancer. 2017;117(10):1478-85.
8. UB P, F T, L B, C G, H E, P T, et al. Magnetic resonance imaging-detected tumor response for locally advanced rectal cancer predicts survival outcomes: MERCURY experience. Journal of clinical oncology : official journal of the American Society of Clinical Oncology. 2011;29(28):3753-60.
9. NJ B, B M, S Y, P T, G B. MR imaging for rectal cancer: the role in staging the primary and response to neoadjuvant therapy. Expert review of gastroenterology & hepatology. 2014;8(6):703-19.
10. Siddiqui MR, Gormly KL, Bhoday J, Balyansikova S, Battersby NJ, Chand M, et al. Interobserver agreement of radiologists assessing the response of rectal cancers to preoperative chemoradiation using the MRI tumour regression grading (mrTRG). Clinical radiology. 2016;71(9):854-62.

11. AM H, L T, Y M, KM W, M G, LB S, et al. Multiparametric MRI in the assessment of response of rectal cancer to neoadjuvant chemoradiotherapy: A comparison of morphological, volumetric and functional MRI parameters. European radiology. 2016;26(12):4303-12.
12. RGH B-T, DMJ L, M M, S B, B B, L C-S, et al. Magnetic resonance imaging for clinical management of rectal cancer: Updated recommendations from the 2016 European Society of Gastrointestinal and Abdominal Radiology (ESGAR) consensus meeting. European radiology. 2018;28(4):1465-75.
13. Yoen H, Park HE, Kim SH, Yoon JH, Hur BY, Bae JS, et al. Prognostic Value of Tumor Regression Grade on MR in Rectal Cancer: A Large-Scale, Single-Center Experience. Korean journal of radiology. 2020;21(9):1065-76.
14. Lambregts DMJ, Yassien AB, Lahaye MJ, Betgen A, Maas M, Beets GL, et al. Monitoring early changes in rectal tumor morphology and volume during 5 weeks of preoperative chemoradiotherapy – An evaluation with sequential MRIs. Radiotherapy and Oncology. 2018;126(3):431-6.
15. LJ W, CD Z, HM Z, YK M, F Y, Y L, et al. The value of MR T2WI signal intensity related parameters for predicting pathological complete response to neoadjuvant chemoradiotherapy in locally advanced rectal cancer. Zhonghua Zhong Liu Za Zhi. 2019;41(11):837-43.
16. L C-S, DM L, M M, T T, RT M, G L, et al. Rectal cancer: assessment of complete response to preoperative combined radiation therapy with chemotherapy–conventional MR volumetry versus diffusion-weighted MR imaging. Radiology. 2011;260(3):734-43.
17. DM L, SX R, S S, MH M, LA H, J B, et al. MRI and Diffusion-weighted MRI Volumetry for Identification of Complete Tumor Responders After Preoperative Chemoradiotherapy in Patients With Rectal Cancer. Ann Surg. 2015;262(6):1034-9.
18. M P, R F, O C, M S, A A, P D, et al. MRI for Assessing Response to Neoadjuvant Therapy in Locally Advanced Rectal Cancer Using DCE-MR and DW-MR Data Sets: A Preliminary Report. BioMed research international. 2015;2015:514740.
19. R VdB, Id-Orcid, JP K, Id-Orcid, B E, M P, et al. Tumor volume regression during preoperative chemoradiotherapy for rectal cancer. Acta Oncol. 2018;57(6):723-7.
20. M I, EM M, O R, ME P. Combined T2w volumetry, DW-MRI and DCE-MRI for response assessment after. Acta Oncol. 2015;54(10):1729-36.
21. Cao W, Li B, Gong J, Hu M, Li W, Pan X, et al. Diffusion-weighted magnetic resonance imaging of mucin pools in locally advanced rectal mucinous adenocarcinoma predicts tumor response to neoadjuvant therapy. European journal of radiology. 2020;125:108890.
22. H N, M L, VR M, T P, M B. Diagnostic Value of Diffusion-Weighted MRI for Tumor Characterization, Differentiation and Monitoring in Pediatric Patients with Neuroblastic Tumors. RoFo : Fortschritte auf dem Gebiete der Rontgenstrahlen und der Nuklearmedizin. 2017;189(7):640-50.
23. TH K, Y H, JJ S, YE C, JH L, WH C. Signal intensity ratio on magnetic resonance imaging as a prognostic factor in patients with cervical compressive myelopathy. Medicine. 2016;95(39):e4649.
24. D H, J L, J B, M R, M O, M M, et al. Image Quality Assessment of 2D versus 3D T2WI and Evaluation of Ultra-high b-Value (b=2,000 mm/s2) DWI for Response Assessment in Rectal Cancer. Anticancer

Res. 2018;38(2):969-78.

25. IM B, GB L, MM G. Quantitative Assessment of Rectal Cancer Response to Neoadjuvant Combined Chemotherapy and Radiation Therapy: Comparison of Three Methods of Positioning Region of Interest for ADC Measurements at Diffusion-weighted MR Imaging. Radiology. 2017;282(2):418-28.
26. SB E, CC C. The American Joint Committee on Cancer: the 7th edition of the AJCC cancer staging manual and the future of TNM. Annals of surgical oncology. 2010;17(6):1471-4.
27. R R, D G, JM H, D T, A W, HE M, et al. Pathological response following long-course neoadjuvant chemoradiotherapy for locally advanced rectal cancer. Histopathology. 2005;47(2):141-6.
28. Kim SH, Chang HJ, Kim DY, Park JW, Baek JY, Kim SY, et al. What Is the Ideal Tumor Regression Grading System in Rectal Cancer Patients after Preoperative Chemoradiotherapy? Cancer research and treatment. 2016;48(3):998-1009.
29. ER D, DM D, DL C-P. Comparing the areas under two or more correlated receiver operating characteristic curves: a nonparametric approach. Biometrics. 1988;44(3):837-45.
30. DMJ L, TN B, RGH B-T. Response evaluation after neoadjuvant treatment for rectal cancer using modern MR imaging: a pictorial review. Insights Imaging. 2019;10(1):019-0706.
31. M M, RAP D, R B-T. Rectal Cancer: Assessing Response to Neoadjuvant Therapy. Magn Reson Imaging Clin N Am. 2020;28(1):117-26.
32. M K, M N, Y K, Y M, T A, M K, et al. Value of intra-tumor heterogeneity evaluated by diffusion-weighted MRI for predicting pathological stages and therapeutic responses to chemoradiotherapy in lower rectal cancer. Journal of Cancer. 2020;11(1):168-76.
33. RAP D, RGH B-T, DMJ L, GL B, M M. Value of DCE-MRI for staging and response evaluation in rectal cancer: A systematic review. European journal of radiology. 2017;95:155-68.
34. AB R, M O, JS B, BE N, B T. Diffusion-weighted imaging of the abdomen at 3.0 Tesla: image quality and Apparent Diffusion Coefficient Reproducibility Compared With 1.5 Tesla. J Magn Reson Imaging. 2011;33(1):128-35.
35. G B, S B, A C, A C, M E, M G, et al. Quality assurance multicenter comparison of different MR scanners for Quantitative Diffusion-Weighted Imaging. J Magn Reson Imaging. 2016;43(1):213-9.

Figures

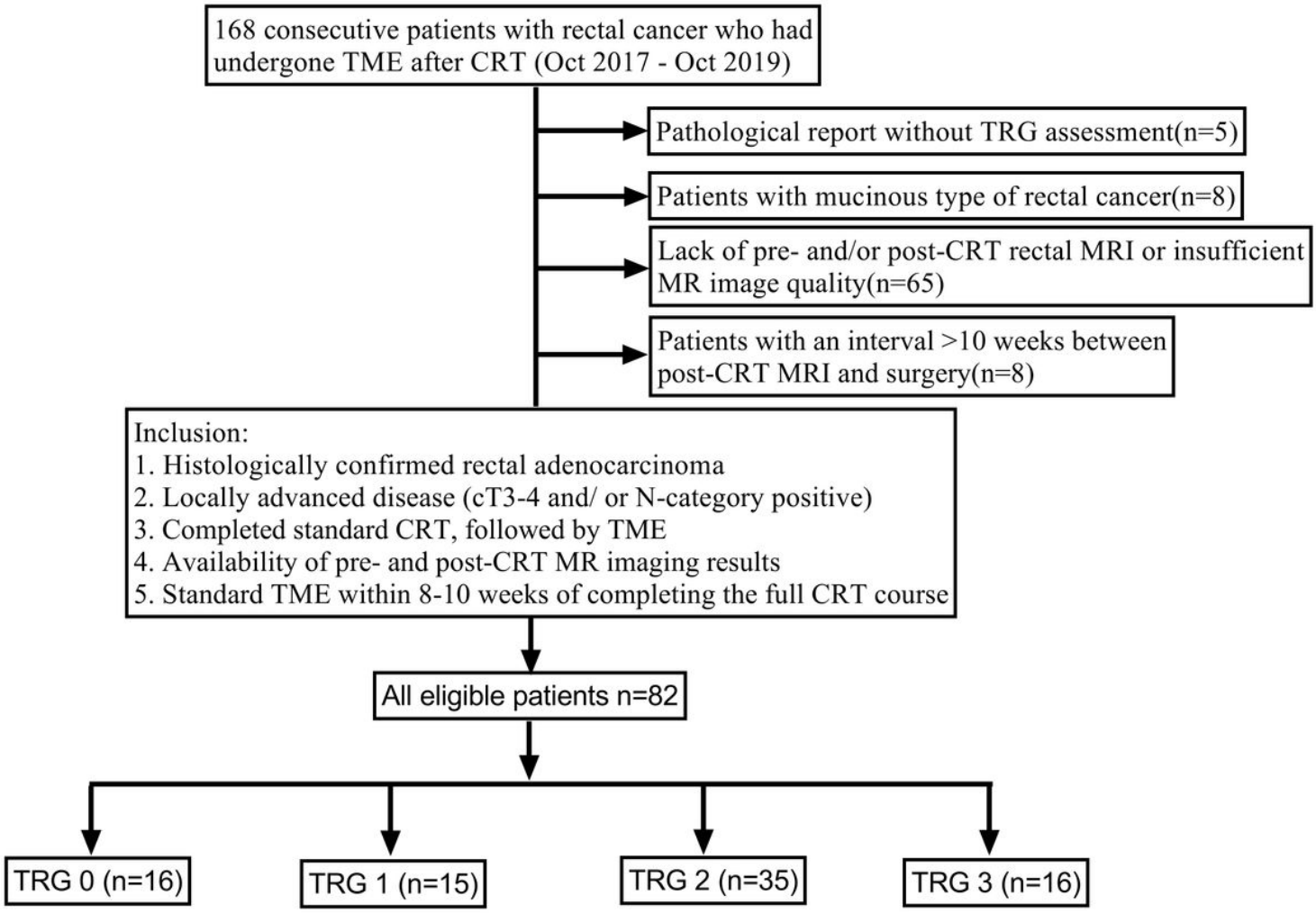

Figure 1

Enrolment and TRG classification of the study population. TME: total mesorectal excision; CRT: chemoradiotherapy; TRG: tumor regression grade; MRI: magnetic resonance imaging.

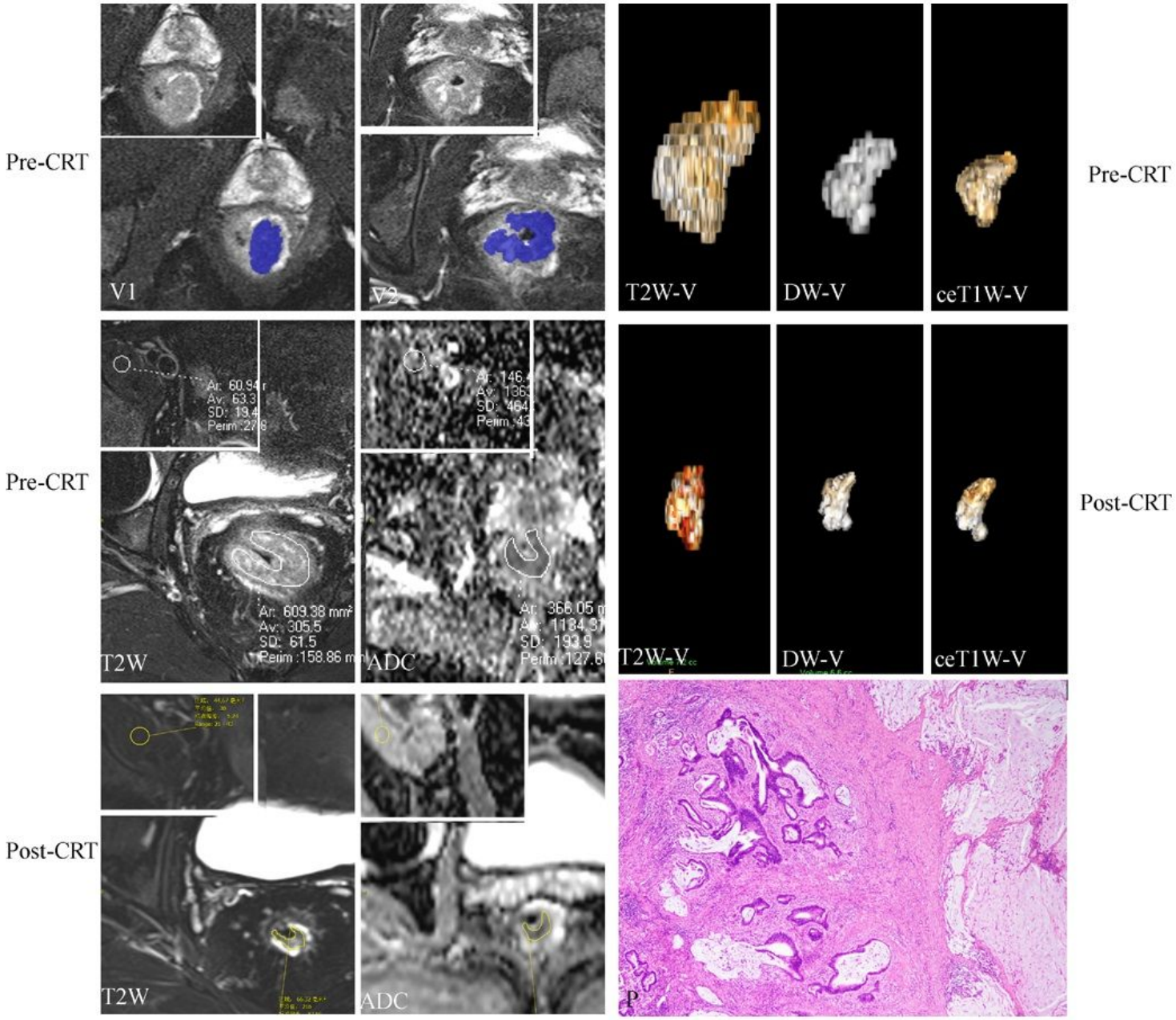

Figure 2

Quantitative volumetric (V) and signal intensity (SI) measurements performed before and after CRT in a representative 63-year-old male patient with LARC who had histologically confirmed moderately differentiated adenocarcinoma stage T4 before CRT, and stage T2 after CRT. Whole-tumor V was calculated by multiplying each cross-sectional area by section thickness (V1–V2). SI of the tumor was measured as the largest relative ROI of cancerous tissue obtained on single same sections of axial T2W, ADC, nonceT1W, and ceTW and from measurements of muscle SI (insets in the upper-left corner). Post-CRT measurements of SI were performed with reference to pre-CRT MRI results to ensure ROIs were placed within same axial level of the primary tumor. The interval between pre- and post-CRT MRI was 115 days, and the interval between post-CRT MRI and surgery was 4 days. Comparison of the pre-CRT and

post-CRT results indicated the tumor changed by 71.08% in T2W-%△2W- , 64.89% in DW-%△V, 68.72% in ceT1W%△V, −27.81% in T2W-%△SIR, and −65.24% in ceT1W-%△SIR. The final histologically analysis confirmed ypT2 and pTRG2.

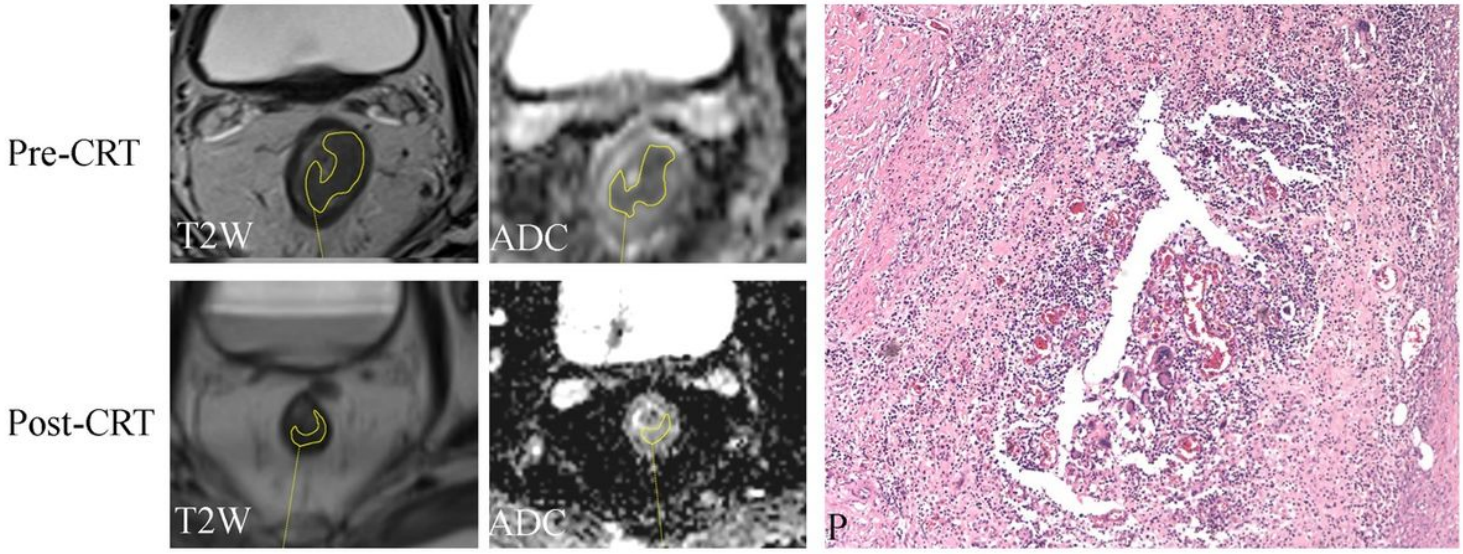

Figure 3

Quantitative signal intensity (SI) measurements performed before and after CRT in a 52-year-old male patient with LARC who had histologically confirmed moderately differentiated adenocarcinoma stage T4 before CRT and stage T2 after CRT. Pre-CRT, the patient had a well-defined, almost circular tumor mass. Post-CRT, tumor SI zones were not identified in the T2W, ADC, nonceT1W, and ceT1W images. The ROIs were positioned at the location of the tumor bed before CRT, based on comparison with pre-CRT MRI results. The interval between pre- and post-CRT MRI was 91 days and the interval between post-CRT MRI and surgery was 9 days. Comparison of the pre-CRT and post-CRT results indicated the tumor changed by 97.77% in T2W-%△V, 94.29% in DW-%△V, 81.37% in ceT1W%4.29% in DW-%△V, 81.ion o and −5.76% in ceT1W-%. The final histological analysis confirmed ypT0 and pTRG0.

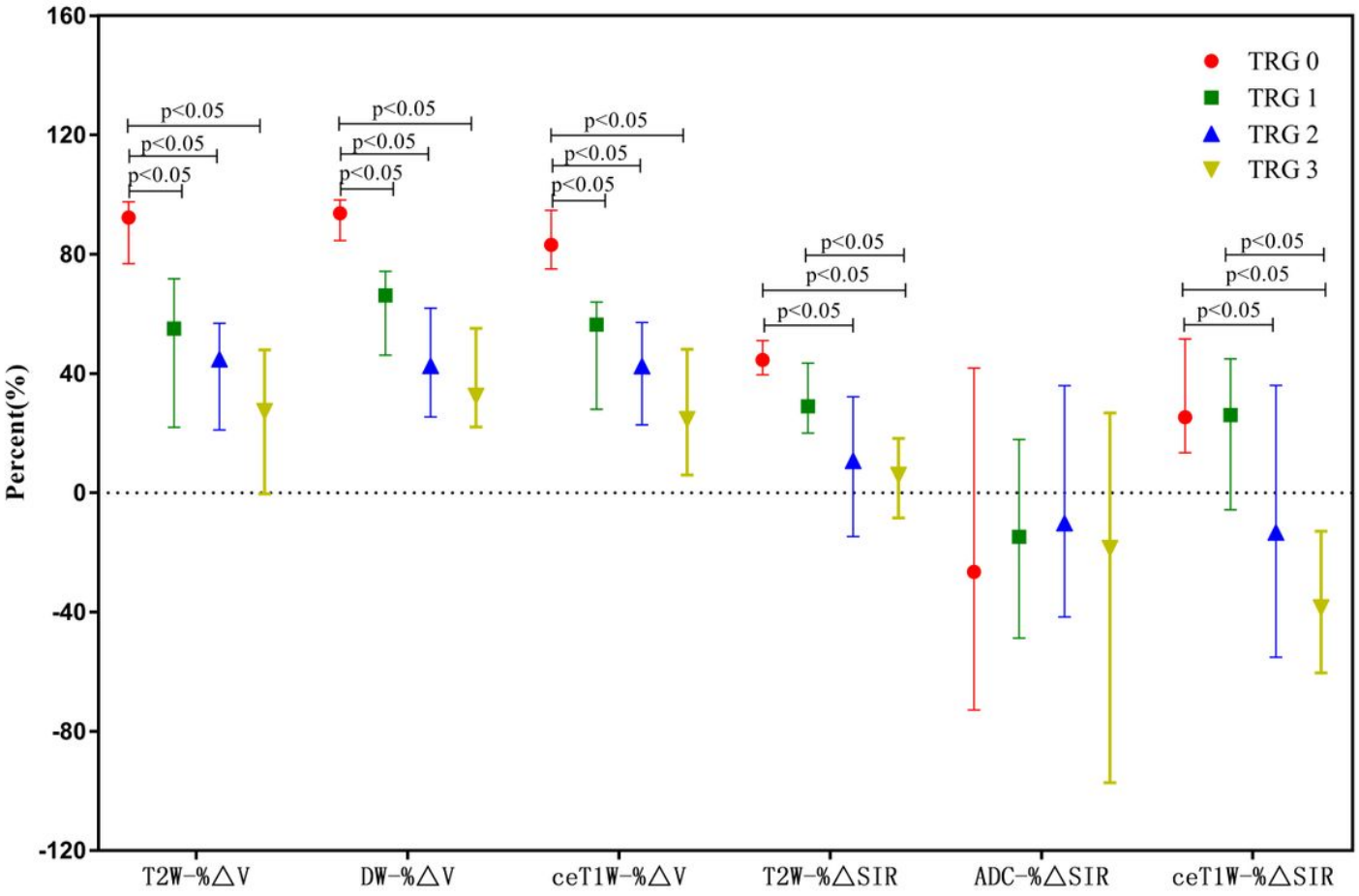

Figure 4

Distribution of %△V and %△SIR in the four TRG groups. Central symbol: median; lower and upper boundaries:25th and 75th percentiles.

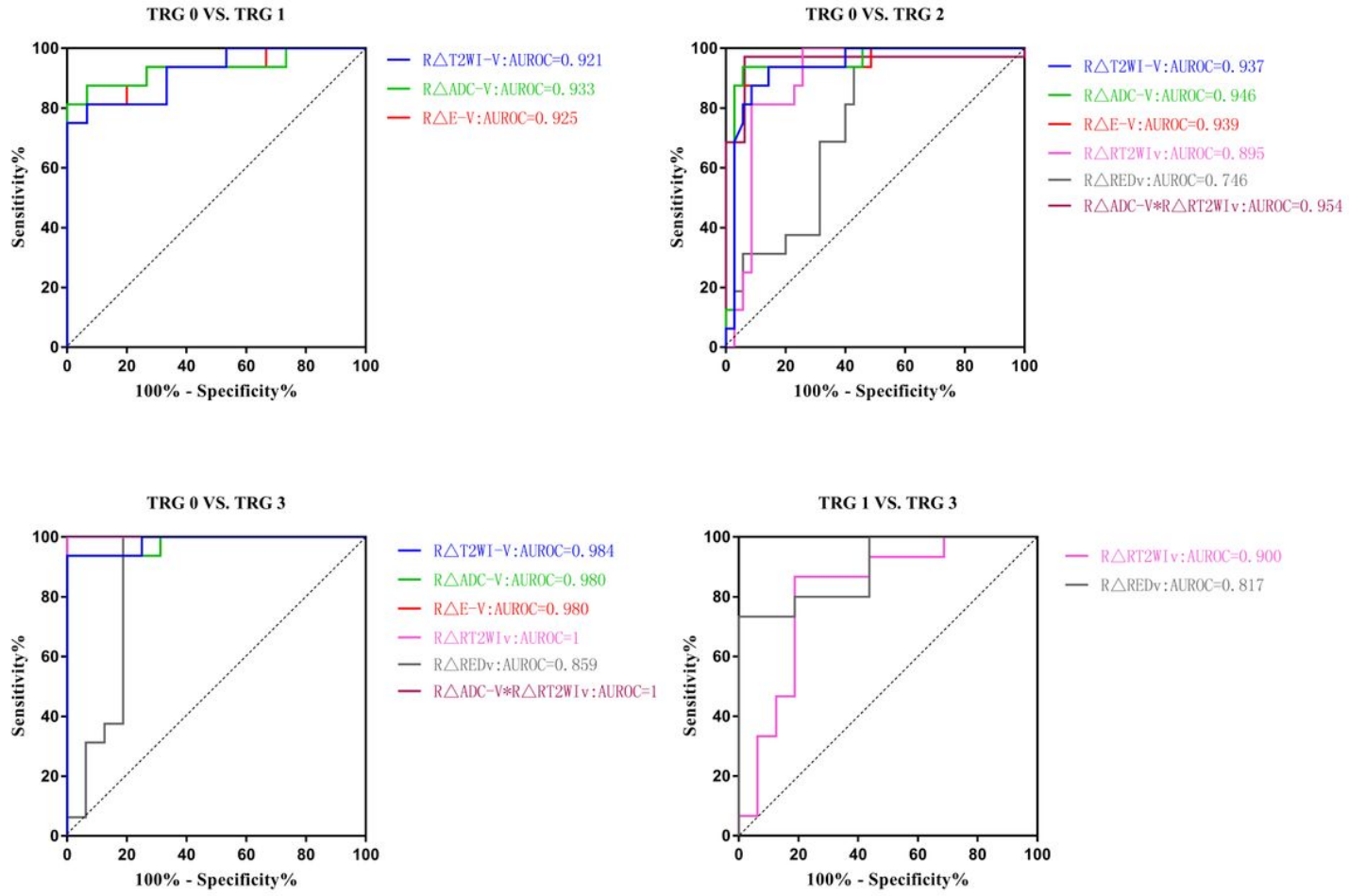

Figure 5

Comparisons of receiver operating characteristic curves determined by %△V and %△SIR from the T1W, ADC/DWI, and ceT1Wsequences for discrimination of different TRGs.

Supplementary Files

This is a list of supplementary files associated with this preprint. Click to download.

- SupplementaryMaterials.docx
- SupplementaryTable.docx